

Switchable wavelength-selective and diffuse metamaterial absorber/emitter with a phase transition spacer layer

Hao Wang, Yue Yang, and Liping Wang

Citation: [Applied Physics Letters](#) **105**, 071907 (2014); doi: 10.1063/1.4893616

View online: <http://dx.doi.org/10.1063/1.4893616>

View Table of Contents: <http://scitation.aip.org/content/aip/journal/apl/105/7?ver=pdfcov>

Published by the [AIP Publishing](#)

Articles you may be interested in

[Wavelength-tunable infrared metamaterial by tailoring magnetic resonance condition with VO₂ phase transition](#)
J. Appl. Phys. **116**, 123503 (2014); 10.1063/1.4896525

[Micro-electro-mechanically switchable near infrared complementary metamaterial absorber](#)
Appl. Phys. Lett. **104**, 201114 (2014); 10.1063/1.4879284

[Demonstration of a nearly ideal wavelength-selective optical mirror using a metamaterial-enabled dielectric coating](#)
Appl. Phys. Lett. **102**, 171114 (2013); 10.1063/1.4804140

[Ultra-thin perfect absorber employing a tunable phase change material](#)
Appl. Phys. Lett. **101**, 221101 (2012); 10.1063/1.4767646

[Gate-field-induced phase transitions in V O 2 : Monoclinic metal phase separation and switchable infrared reflections](#)
Appl. Phys. Lett. **93**, 171101 (2008); 10.1063/1.3009569

The advertisement features a red and white color scheme. On the left, text reads 'Confidently measure down to 0.01 fA and up to 10 PΩ' and 'Keysight B2980A Series Picoammeters/Electrometers'. A red button with white text says 'View video demo >'. On the right, there is an image of the Keysight B2980A device and the Keysight Technologies logo.

Switchable wavelength-selective and diffuse metamaterial absorber/emitter with a phase transition spacer layer

Hao Wang, Yue Yang, and Liping Wang^{a)}

School for Engineering of Matter, Transport and Energy, Arizona State University, Tempe, Arizona 85287, USA

(Received 19 May 2014; accepted 9 August 2014; published online 19 August 2014)

We numerically demonstrate a switchable metamaterial absorber/emitter by thermally turning on or off the excitation of magnetic resonance upon the phase transition of vanadium dioxide (VO_2). Perfect absorption peak exists around the wavelength of $5\ \mu\text{m}$ when the excitation of magnetic resonance is supported with the insulating VO_2 spacer layer. The wavelength-selective absorption is switched off when the magnetic resonance is disabled with metallic VO_2 that shorts the top and bottom metallic structures. The resonance wavelength can be tuned with different geometry, and the switchable metamaterial exhibits diffuse behaviors at oblique angles. The results would facilitate the design of switchable metamaterials for active control in energy and sensing applications.

© 2014 AIP Publishing LLC. [<http://dx.doi.org/10.1063/1.4893616>]

Great progresses have been made on both selective absorbers and thermal emitters in the past decade, and enormous applications like radiative cooling,¹ sensing,² and energy conversion systems^{3,4} have been found. Selective absorption has been achieved in a wide range from THz to visible. Tao *et al.*⁵ demonstrated 70% absorption at 1.3 THz with a metamaterial design consisting of a bilayer unit cell. Chen *et al.*⁶ proposed a dual-band selective absorber for infrared spectroscopy. By shrinking the feature size of structures, selective absorption has been obtained in the visible range for the applications like solar absorption and light trapping.^{7–9} On the other hand, a great number of selective emitters have been designed for energy-related applications. Wang *et al.*¹⁰ investigated a selective emitter made of a photonic crystal structure sandwiched by SiC gratings. Arnold *et al.*¹¹ demonstrated two-dimensional (2D) selective emitters by exciting surface phonon polaritons in SiC gratings. Argyropoulos *et al.*¹² promoted a selective emitter based on plasmonic Brewster metasurfaces. Shu *et al.*¹³ showed a selective emitter constructed by porous metal-based multilayers. In addition, selective absorbers/emitters made of film-coupled plasmonic metamaterials by exciting magnetic resonance were also studied.^{14–18}

One concern is that all aforementioned structures are static, while active control in the selective absorption or emission is highly beneficial in practical applications. Recent efforts have been made in actively tuning material radiative properties. Shrekenhamer *et al.*¹⁹ proposed a liquid crystal based metamaterial with tunable absorption in THz by applying external electric field to change the optical properties of liquid crystal. Thongrattanasiri *et al.*²⁰ proved selective absorption in the infrared through periodically patterned graphene structures, and the absorption is tuned via electrostatic doping of graphene. Cong *et al.*²¹ discussed potential of split-ring resonator as a tunable selective absorber by use of InSb, whose carrier density can be adjusted by utilizing optical pumping or changing surrounding temperature.

Vanadium dioxide (VO_2) has been known for its phase transition at temperature of $68\ ^\circ\text{C}$, above which it is an isotropic metal or a uniaxial insulator otherwise.^{22,23} Tunable metamaterial absorbers in the microwave²⁴ and THz regimes²⁵ were designed by using VO_2 film as the ground plane to modulate the impedance match conditions for splitting resonators (SRRs). Dicken *et al.*²⁶ reported a metamaterial with tunable resonance frequency in the near-infrared by depositing SRRs on a continuous VO_2 film, which modulates surface plasmon at different phases. Similarly, a thermally tunable mid-infrared metamaterial made of a Y-shape plasmonic antenna array on a VO_2 film was demonstrated.²⁷ Besides, Ben-Abdallah *et al.*²⁸ proposed a phase-change thermal antenna made of patterned VO_2 gratings that exhibits switchable thermal emission enabled by surface plasmon polaritons excited only at the metallic phase of VO_2 .

In this work, we propose a switchable metamaterial absorber/emitter by turning on or off the excitation of magnetic resonance using a VO_2 spacer layer upon its phase transition. Figure 1(a) depicts the proposed structure, which consists of a 1D gold grating with period $\Lambda = 1\ \mu\text{m}$, stripe width $w = 0.5\ \mu\text{m}$, and height $h = 80\ \text{nm}$ on a gold film separated by a thin VO_2 spacer layer with thickness $d = 80\ \text{nm}$. The bottom Au film could be as thin as $100\ \text{nm}$ as long as it is optically opaque. Here, the phase transition of VO_2 is driven by a temperature-controlled stage, which the structure is placed upon, while the heating or cooling could be realized by different means in a particular application.

The finite-difference time-domain (FDTD) method (Lumerical Solutions, Inc.) was employed to numerically calculate the spectral-directional reflectance R , from which the spectral-directional absorptance of the metamaterial structure was obtained as $\alpha = 1 - R$. A unit cell with a domain size of $1\ \mu\text{m} \times 1\ \mu\text{m} \times 6\ \mu\text{m}$ was simulated, and sufficiently fine meshes were used to ensure the numerical convergence. Periodic boundary condition was used in both x and y directions at normal incidence, while Bloch boundary condition was implemented at oblique incidence. Perfect matched layers with reflection coefficients less than 10^{-6}

^{a)}E-mail: liping.wang@asu.edu. Tel: 1-480-727-8615.

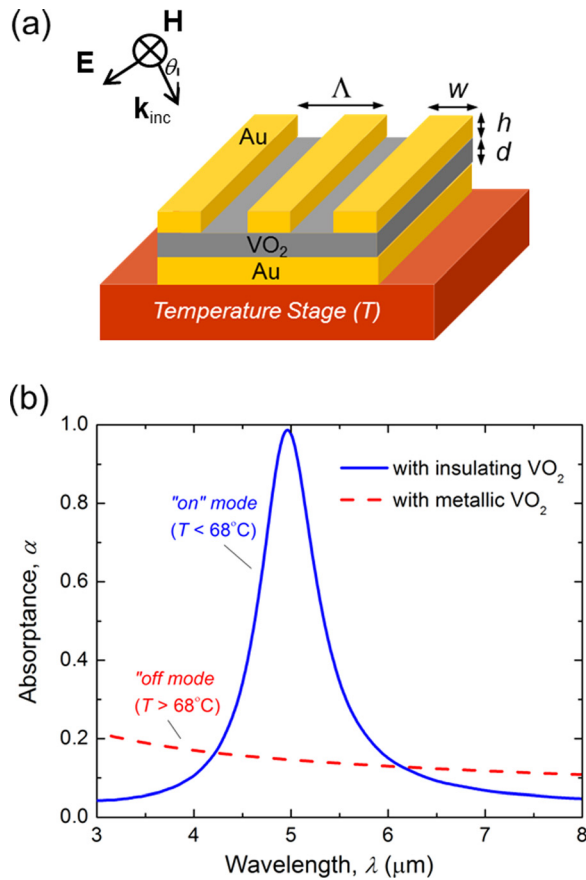


FIG. 1. (a) Schematic of the proposed switchable metamaterial absorber/emitter made of one-dimensional gold grating (period $\Lambda = 1 \mu\text{m}$, stripe width $w = 0.5 \mu\text{m}$, and height $h = 80 \text{nm}$), a thin VO_2 layer (thickness $d = 80 \text{nm}$), and an opaque bottom gold substrate. (b) Spectral absorbance of the switchable metamaterial at normal incidence and TM-wave polarization upon phase transition of VO_2 at 68°C , suggesting the “on” and “off” modes.

were applied in z direction. The transverse magnetic (TM) waves, at which the magnetic field \mathbf{H} is parallel to the grating grooves, were considered here because magnetic resonance can be excited only under this polarization in 1D grating structures.^{14,15} The optical properties of gold were taken from Palik.²⁹ The dielectric function of the metallic VO_2 was obtained from a Drude model, while the insulating phase was modeled as a uniaxial medium with a dielectric function tensor²²

$$\bar{\epsilon}_{\text{insulator}} = \begin{pmatrix} \epsilon_O & 0 & 0 \\ 0 & \epsilon_O & 0 \\ 0 & 0 & \epsilon_E \end{pmatrix}, \quad (1)$$

where ϵ_O and ϵ_E are the ordinary (i.e., when incident electric field is perpendicular to its optical axis) and extraordinary (i.e., when incident electric field is parallel to its optical axis) components, respectively. Note that only ϵ_O plays a role at normal incidence, while ϵ_E has to be considered at oblique incidence.³⁰

Figure 1(b) shows the spectral absorbance of the metamaterial structure at normal incidence in the mid-infrared regime from $3 \mu\text{m}$ to $8 \mu\text{m}$ in wavelength upon VO_2 phase transition. When the structure temperature is below 68°C , i.e., VO_2 is at dielectric phase, a large absorption peak occurs

with perfect absorption at $\lambda_{\text{max}} = 4.96 \mu\text{m}$. The full width at half maximum (FWHM) for this peak is $\Delta\lambda = 0.72 \mu\text{m}$, resulting in a quality factor of 6.89, defined by $Q = \lambda_{\text{max}}/\Delta\lambda$. However, when the temperature is further increased beyond the phase transition temperature, VO_2 turns into metal and the absorption peak disappears with absorptance less than 0.15 at the same wavelength. The structure essentially becomes reflective in the considered mid-infrared regime. Therefore, simply by controlling the temperature below or above 68°C , the absorption peak around $5 \mu\text{m}$ could be turned “on” or “off,” suggesting a switchable selective metamaterial absorber upon VO_2 phase transition. It is worth noting that the spectral-directional absorptance is equal to spectral-directional emittance, according to Kirchhoff’s law. Therefore, such a metamaterial structure could potentially be a switchable infrared thermal emitter, which would find applications in space cooling, building energy management, and energy-efficient light sources.

To illustrate the underlying mechanism for the switchable metamaterial absorber/emitter, the electromagnetic field distributions at the peak absorption wavelength $\lambda_{\text{max}} = 4.96 \mu\text{m}$ were plotted at the “on” and “off” modes, respectively, shown in Figs. 2(a) and 2(b). The cross section of two unit cells was presented with the top gold grating, VO_2 layer and bottom gold film delineated. The arrows represent the electric field vectors, while the background contour indicates the relative strength of magnetic field to the incidence as $\log_{10}|H/H_0|^2$.

As seen in Fig. 2(a), in which the VO_2 is at its dielectric phase, strong magnetic field energy with two orders of

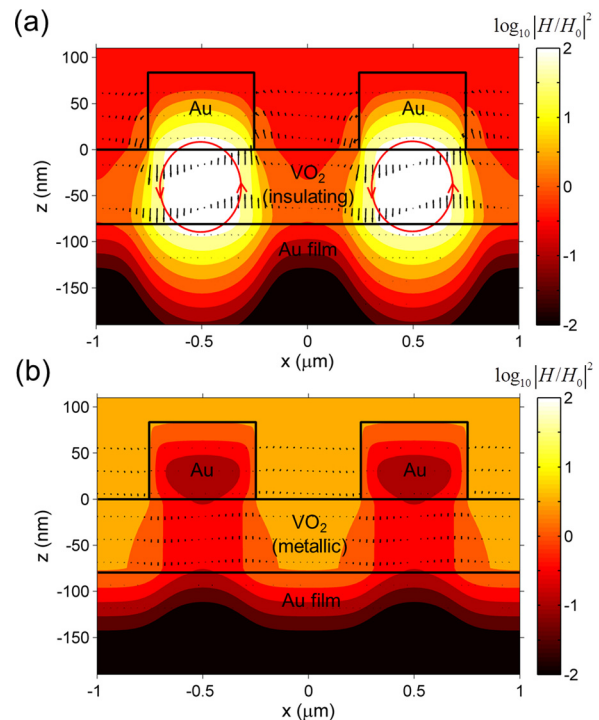


FIG. 2. Electromagnetic field distributions at the peak wavelength $\lambda_{\text{max}} = 4.96 \mu\text{m}$ in the switchable metamaterial with VO_2 at the (a) dielectric phase and (b) metallic phase. The magnetic resonance is excited with dielectric VO_2 , resulting in strong field confinement and thus absorption, while it is turned off when VO_2 becomes metallic.

magnitude larger than the incidence is localized inside the insulating VO₂ layer between top and bottom gold layers, which is responsible for the strong resonant absorption at this particular wavelength. Moreover, the electric field vectors around the localized magnetic field suggest a current loop. This is the exact behavior when magnetic resonance is excited, which has been previously studied in the similar metamaterial structures with metal-insulator-metal configurations.^{14–17}

When magnetic resonance is excited, anti-parallel electric currents are formed around the antinode of the localized magnetic field. The anti-parallel electric currents are due to the non-uniform charge distribution within the metal surfaces at the top and bottom of the dielectric VO₂ spacer. Charges with opposite signs accumulate at the left and right edges of the gold strip and the bottom gold film across the dielectric spacer. When the VO₂ is a dielectric, the charges form a capacitor C_m between top and bottom metals, while the metals serve as inductors, as illustrated in Fig. 3(a). The existence of the capacitor with the insulating VO₂ is critical in this inductor-capacitor (LC) circuit to excite the magnetic resonance at a particular wavelength.

However, as shown in Fig. 2(b) when the VO₂ becomes metallic, the strong magnetic field confinement disappears, which results in the absorption peak to be switched “off.” This can be explained by the fact that the capacitor C_m can be no longer formed when VO₂ is metallic. In other words,

the top and bottom metals are shorted by the metallic VO₂ such that charges with opposite signs cannot accumulate across the VO₂ spacer layer to form a capacitor. Without a capacitor, the resonance of an LC circuit cannot be excited.

To further explain the underlying physics, detailed analysis with the LC model is presented here. Based on the insights gained from the electromagnetic field distribution on the charge distribution, the top and bottom metals can be treated as inductors, which include two components as mutual inductance L_m and kinetic inductance L_k per unit length along the grating groove direction with the expressions as^{14,15}

$$L_m = 0.5\mu_0 wd, \quad (2)$$

$$L_k = -\frac{w}{\omega^2 \epsilon_0 \epsilon'_{Au} \delta_{Au}}, \quad (3)$$

where μ_0 is the magnetic permeability of vacuum, ϵ_0 is the electric permittivity for vacuum, ω is the angular frequency, ϵ'_{Au} is the real part of the permittivity of bulk gold, and δ_{Au} is the penetration depth of bulk gold. The insulating VO₂ spacer helps to form a parallel-plate capacitor C_m , which can be expressed as^{14,15}

$$C_m = \frac{c_1 \epsilon_0 \epsilon_d w}{d}, \quad (4)$$

where $c_1 = 0.22$ is the coefficient that accounts for non-uniform charge distribution at the metal surfaces, and ϵ_d is the permittivity of insulating VO₂, which has to be positive. Metallic VO₂ possesses a negative permittivity, which fails to form a capacitor.³⁰ The magnetic resonance occurs when the impedance of the LC circuit becomes zero, which results in the resonance condition to be determined by

$$\lambda_{MR} = 2\pi c_0 \sqrt{(L_m + L_k)C_m}. \quad (5)$$

For the structure with insulating VO₂ considered in Fig. 1(b), the LC model predicts the magnetic resonance to occur at $\lambda_{MR} = 4.86 \mu\text{m}$, which yields a 2% relative error compared to the FDTD simulation. Similar LC circuit models have been successfully employed to verify the physical mechanism and predict the magnetic resonance conditions in plasmonic metamaterials.^{31–33} It is worth mentioning that there is an additional capacitance, called gap capacitance C_g , which considers the electromagnetic coupling between the neighboring gold stripes.^{14,15} However, calculation showed that C_g is less than 2% of C_m in the present study and thus is reasonably neglected here.

Figure 3(b) presents the contour plot of the normal absorptance of the proposed switchable metamaterial as a function of wavelength and stripe width when it is at the “on” mode with insulating VO₂. The bright contour band indicates the absorption peak associated with the excitation of magnetic resonance. It is clearly seen that, the resonance peak shifts to longer wavelengths when the stripe width increases from $0.3 \mu\text{m}$ to $0.8 \mu\text{m}$, suggesting that the peak could be easily tuned to obtain the selective absorption at desired wavelengths by varying different geometric values during the structure design process, to meet different application needs.

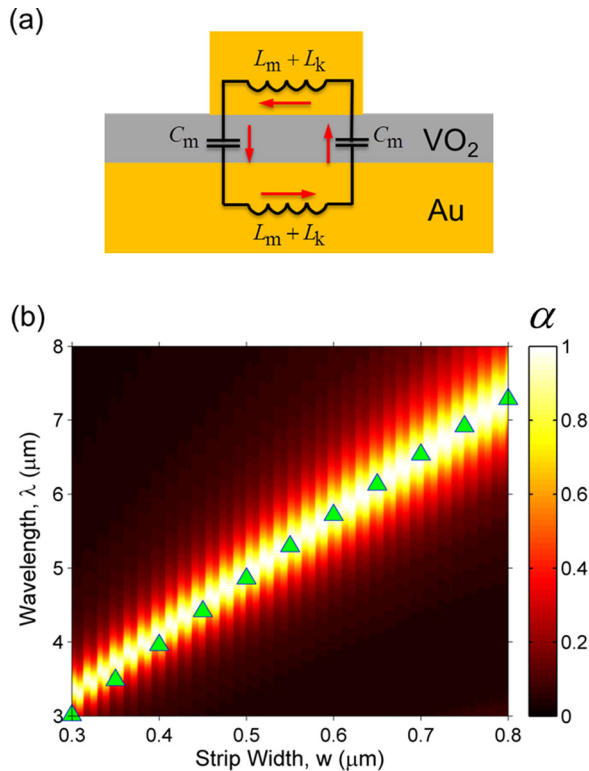


FIG. 3. (a) Schematic of the LC model that explains the physical mechanism of the switchable absorption peak due to excitation of magnetic resonance upon VO₂ phase transition. (b) Contour plot of normal absorptance as a function of wavelength and stripe width of the switchable metamaterial at the “on” mode. The predicted condition for magnetic resonance from the LC model is shown as triangular markers.

The predicted resonance wavelengths from the LC model were also plotted as triangular markers for comparison, which match well with the resonance band from the FDTD simulation, undoubtedly confirming the underlying physics as magnetic resonance. The geometric dependence of the resonance wavelength is also clearly suggested from the inductance and capacitance expressions. When stripe width w increases, L_m , L_k , and C_m will become larger according to Eqs. (2)–(4), and thereby the resonance wavelength from Eq. (5) increases.

The behavior of the switchable metamaterial absorber/emitter at oblique angles is also important for sensing and energy related applications. The absorption or emission associated with excitation of magnetic resonance has been demonstrated with angular independent behaviors, but previously studied metamaterial structures were made of isotropic materials.^{14,15,17} In our proposed structure, the insulating VO₂ is a uniaxial medium and exhibits anisotropic optical behaviors at oblique incidences. The effect of VO₂ anisotropy on the magnetic resonance and the radiative properties of the switchable metamaterial absorber/emitter needs to be studied and understood.

Figure 4 plots the directional absorptance of the switchable metamaterial with insulating VO₂ at the magnetic resonance wavelength of $\lambda_{\max} = 4.96 \mu\text{m}$ in the hemisphere with the incident angle varying from -85° to 85° at TM polarization from the FDTD simulation. The absorptance remains near unity from normal direction to $\theta = 30^\circ$, slightly decreases to 0.83 at $\theta = 60^\circ$, and then drops quickly when it approaches the grazing angle. Surprisingly, the phase-change metamaterial absorber still exhibits strong diffuse behavior at the absorption peak even though the insulating VO₂ is anisotropic at oblique angles. This can be explained by the insignificant difference between the ordinary and extraordinary dielectric functions of insulating VO₂.³⁰ Materials with larger anisotropy like hyperbolic metamaterials might affect more the radiative properties at oblique angles.³⁴

In conclusion, we have demonstrated a switchable metamaterial absorber/emitter by thermally turning on or off the excitation of magnetic resonance upon the phase transition of VO₂. A perfect absorption peak exists selectively around $\lambda = 5 \mu\text{m}$ when the VO₂ is at the insulating phase, and the peak wavelength can be easily tuned with different stripe width. The absorption peak disappears when the VO₂ is metallic by increasing the temperature beyond the phase transition at 68°C . Note that the phase transition temperature of

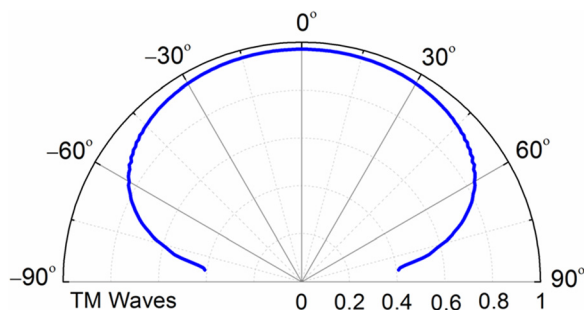


FIG. 4. Polar plot of the directional absorptance of the switchable metamaterial at the “on” mode with insulating VO₂ as a function of incident angle at the peak wavelength ($\lambda = 4.96 \mu\text{m}$) under TM-wave incidence.

VO₂ can be tuned through doping^{35,36} for applications that require different switching temperatures. The underlying mechanism is explained in detail as the excitation of magnetic resonance with the help of electromagnetic field plots and the LC circuit model. Diffuse behavior of the switchable metamaterial is also demonstrated at oblique angles for TM waves. Polarization-independent switchable absorber/emitters could be realized with symmetric 2D grating structures.^{16,17} The results would facilitate the design and application of a new class of switchable metamaterials in active thermal control for building and space cooling, as well as active thermal detectors.

This work was supported by the New Faculty Startup fund at Arizona State University.

- ¹E. Rephaeli, A. Raman, and S. Fan, *Nano Lett.* **13**, 1457 (2013).
- ²A. Tittl, P. Mai, R. Taubert, D. Dregely, N. Liu, and H. Giessen, *Nano Lett.* **11**, 4366 (2011).
- ³I. Celanovic, N. Jovanovic, and J. Kassakian, *Appl. Phys. Lett.* **92**, 193101 (2008).
- ⁴I. Massiot, C. Colin, N. Péré-Laperne, P. R. i Cabarrocas, C. Sauvan, P. Lalanne, J.-L. Pelouard, and S. Collin, *Appl. Phys. Lett.* **101**, 163901 (2012).
- ⁵H. Tao, N. I. Landy, C. M. Bingham, X. Zhang, R. D. Averitt, and W. J. Padilla, *Opt. Express* **16**, 7181 (2008).
- ⁶K. Chen, R. Adato, and H. Altug, *ACS Nano* **6**, 7998 (2012).
- ⁷K. Aydin, V. E. Ferry, R. M. Briggs, and H. A. Atwater, *Nat. Commun.* **2**, 517 (2011).
- ⁸A. Moreau, C. Ciraci, J. J. Mock, R. T. Hill, Q. Wang, B. J. Wiley, A. Chilkoti, and D. R. Smith, *Nature* **492**, 86 (2012).
- ⁹L.-H. Zhu, M.-R. Shao, R.-W. Peng, R.-H. Fan, X.-R. Huang, and M. Wang, *Opt. Express* **21**, A313 (2013).
- ¹⁰W. Wang, C. Fu, and W. Tan, *J. Quant. Spectrosc. Radiat. Transfer* **132**, 36 (2014).
- ¹¹C. Arnold, F. Marquier, M. Garin, F. Pardo, S. Collin, N. Bardou, J.-L. Pelouard, and J.-J. Greffet, *Phys. Rev. B* **86**, 035316 (2012).
- ¹²C. Argyropoulos, K. Q. Le, N. Mattiucci, G. D’Aguanno, and A. Alù, *Phys. Rev. B* **87**, 205112 (2013).
- ¹³S. Shu, L. Zheng, H. Li, C. K. Tsang, L. Shi, and Y. Y. Li, *Opt. Lett.* **37**, 4883 (2012).
- ¹⁴B.-J. Lee, L. P. Wang, and Z. M. Zhang, *Opt. Express* **16**, 11328 (2008).
- ¹⁵L. P. Wang and Z. M. Zhang, *Appl. Phys. Lett.* **100**, 063902 (2012).
- ¹⁶B. Zhao, L. P. Wang, Y. Shuai, and Z. M. Zhang, *Int. J. Heat Mass Transfer* **67**, 637 (2013).
- ¹⁷H. Wang and L. P. Wang, *Opt. Express* **21**, A1078 (2013).
- ¹⁸H. Wang, K. O’Dea, and L. P. Wang, *Opt. Lett.* **39**, 1457 (2014).
- ¹⁹D. Shrekenhamer, W.-C. Chen, and W. J. Padilla, *Phys. Rev. Lett.* **110**, 177403 (2013).
- ²⁰S. Thongrattanasiri, F. H. Koppens, and F. J. G. de Abajo, *Phys. Rev. Lett.* **108**, 047401 (2012).
- ²¹J. Cong, B. Yun, and Y. Cui, *Opt. Express* **21**, 20363 (2013).
- ²²A. Barker, Jr., H. Verleur, and H. Guggenheim, *Phys. Rev. Lett.* **17**, 1286 (1966).
- ²³M. M. Qazilbash, M. Brehm, B.-G. Chae, P.-C. Ho, G. O. Andreev, B.-J. Kim, S. J. Yun, A. V. Balatsky, M. B. Maple, F. Keilmann, H.-T. Kim, and D. N. Basov, *Science* **318**, 1750 (2007).
- ²⁴Q.-Y. Wen, H.-W. Zhang, Q.-H. Yang, Z. Chen, Y. Long, Y.-L. Jing, Y. Lin, and P.-X. Zhang, *J. Phys. D: Appl. Phys.* **45**, 235106 (2012).
- ²⁵J.-N. Li, W. Li, and S.-J. Chang, *J. Electron. Sci. Technol.* **1**, 009 (2014).
- ²⁶M. J. Dicken, K. Aydin, I. M. Pryce, L. A. Sweatlock, E. M. Boyd, S. Walavalkar, J. Ma, and H. A. Atwater, *Opt. Express* **17**, 18330 (2009).
- ²⁷M. A. Kats, R. Blanchard, P. Genevet, Z. Yang, M. M. Qazilbash, D. Basov, S. Ramanathan, and F. Capasso, *Opt. Lett.* **38**, 368 (2013).
- ²⁸P. Ben-Abdallah, H. Benisty, and M. Besbes, *J. Appl. Phys.* **116**, 034306 (2014).
- ²⁹E. D. Palik, *Handbook of Optical Constants of Solids* (Academic Press, 1985).
- ³⁰Y. Yang, S. Basu, and L. P. Wang, *Appl. Phys. Lett.* **103**, 163101 (2013).

- ³¹J. Zhou, E. N. Economou, T. Koschny, and C. M. Soukoulis, *Opt. Lett.* **31**, 3620 (2006).
- ³²F. Costa, S. Genovesi, A. Monorchio, and G. Manara, *IEEE Trans. Antennas Propag.* **61**, 1201 (2013).
- ³³A. Isenstadt and J. Xu, *Electron. Mater. Lett.* **9**, 125 (2013).
- ³⁴C. Cortes, W. Newman, S. Molesky, and Z. Jacob, *J. Opt.* **14**, 063001 (2012).
- ³⁵L. Q. Mai, B. Hu, T. Hu, W. Chen, and E. D. Gu, *J. Phys. Chem. B* **110**, 19083 (2006).
- ³⁶X. Tan, T. Yao, R. Long, Z. Sun, Y. Feng, H. Cheng, X. Yuan, W. Zhang, Q. Liu, C. Wu, Y. Xie, and S. Wei, *Sci. Rep.* **2**, 466 (2012).